Analysis of the $\Lambda_b \to \Lambda_c + l\bar{\nu}_l$ decay within a light-front constituent quark model

Fabio Cardarelli and Silvano Simula*
Istituto Nazionale di Fisica Nucleare, Sezione Roma III, Via della Vasca Navale 84, I-00146 Roma, Italy
(Received 19 October 1998; published 8 September 1999)

We present an investigation of the Isgur-Wise form factor relevant for the semileptonic decay $\Lambda_b \to \Lambda_c + l\bar{\nu}_l$ performed within a light-front constituent quark model. Adopting different baryon wave functions it is found that the Isgur-Wise form factor depends sensitively on the baryon structure. It is shown however that the shape of the Isgur-Wise function in the full recoil range relevant for the $\Lambda_b \to \Lambda_c + l\bar{\nu}_l$ decay can be effectively constrained using recent lattice QCD results at low recoil. Then the $\Lambda_b \to \Lambda_c + l\bar{\nu}_l$ decay is investigated including both radiative effects and first-order power corrections in the inverse heavy-quark mass. Our final predictions for the exclusive semileptonic branching ratio, the longitudinal and transverse asymmetries, and the longitudinal to transverse decay ratio are $Br(\Lambda_b \to \Lambda_c l\bar{\nu}_l) = (6.3 \pm 1.6)\% \, |V_{bc}/0.040|^2 \tau(\Lambda_b)/(1.24\,\text{ps})$, $a_L = -0.945 \pm 0.014$, $a_T = -0.62 \pm 0.09$ and $R_{L/T} = 1.57 \pm 0.15$, respectively. Moreover, both the longitudinal asymmetry and the (partially integrated) longitudinal to transverse decay ratio are found to be only marginally affected by the model dependence of the Isgur-Wise form factor as well as by first-order power corrections; therefore, their experimental determination might be a very interesting tool for testing the SM and for investigating possible new physics. [S0556-2821(99)06817-4]

PACS number(s): 12.38.Lg, 12.39.Ki, 13.30.Ce, 14.20.Mr

I. INTRODUCTION

The heavy quark effective theory (HQET) is widely recognized as an appropriate theoretical framework for analyzing the properties of baryons containing a single heavy quark (Q). It provides a systematic expansion of the QCD Lagrangian as a series of powers of the inverse heavy-quark mass (m_Q). At the leading order a new spin-flavor symmetry, called heavy quark symmetry (HQS), arises. Such a symmetry is shared by, but not manifest in QCD and it is broken by radiative corrections as well as by nonperturbative contributions, which can be organized as an expansion in powers of $1/m_Q$. The HQS allows one to derive several model-independent relations among hadronic properties and, in particular, all the electroweak transition and elastic amplitudes can be expressed in terms of a subset of *universal* form factors [1]. In the case of the semileptonic decay process $\Lambda_b \to \Lambda_c + l\bar{\nu}_l$ the vector and axial-vector transition amplitudes, $\langle \Lambda_c(v')|\bar{c}\gamma^\mu b|\Lambda_b(v)\rangle$ and $\langle \Lambda_c(v')|\bar{c}\gamma^\mu\gamma^5 b|\Lambda_b(v)\rangle$, where $v(v')$ is the initial (final) baryon four-velocity, can be expressed in terms of only one universal function [1], called the Isgur-Wise (IW) form factor $\xi(\omega)$, where $\omega \equiv v \cdot v'$. However, except for the normalization condition $\xi(1)=1$, the HQS cannot predict the full behavior of the IW form factor, for the complete knowledge of the nonperturbative baryon structure is required. Therefore, calculations based on lattice QCD simulations, effective approaches and models are necessary in order to obtain reliable quantitative predictions, which could allow to extract from the data important information on fundamental parameters, such as e.g., the Cabibbo-Kobayashi-Maskawa (CKM) weak mixing angles, and on possible extensions of the standard model (SM).

In this work we adopt a relativistic constituent quark model formulated on the light-front (LF), and, using different types of Qqq' wave functions (where q and q' are two light spectator quarks), we extend our investigation started in Ref. [2] concerning the IW form factor $\xi(\omega)$ relevant for the decay process $\Lambda_b \to \Lambda_c + l\bar{\nu}_l$. Our aim is to constrain as much as possible the model dependence of the calculated IW form factor in order to estimate several observables, like the exclusive semileptonic branching ratio and various (integrated) asymmetries. To this end we will make use of recent lattice QCD simulations [3] at low recoil, so that our model can be viewed as a lattice-constrained LF quark model. After including both radiative effects and first-order $1/m_Q$ corrections to the relevant form factors, our final results for the exclusive semileptonic branching ratio, the longitudinal and transverse asymmetries, and the longitudinal to transverse decay ratio are $Br(\Lambda_b \to \Lambda_c l\bar{\nu}_l) = (6.3 \pm 1.6)\% |V_{bc}/0.040|^2 \tau(\Lambda_b)/(1.24\ \text{ps})$, $a_L = -0.945 \pm 0.014$, $a_T = -0.62 \pm 0.09$ and $R_{L/T} = 1.57 \pm 0.15$, respectively. The theoretical uncertainties on $Br(\Lambda_b \to \Lambda_c l\bar{\nu}_l)$ and $R_{L/T}$ can be significantly reduced to $\simeq 12\%$ and $\simeq 1\%$, respectively, by integrating the differential decay rates up to $\omega \simeq 1.2$. This could allow in particular to extract the CKM matrix elements $|V_{bc}|$ with a theoretical uncertainty of $\simeq 6\%$, which is comparable with present uncertainties obtained from exclusive semileptonic B-meson decays [4].

We want to point out that our estimates of the theoretical errors include the uncertainties arising both from the model dependence of the IW form factor and the first-order power corrections. In the case of the longitudinal asymmetry and the (partially integrated) longitudinal to transverse decay ratio our uncertainties turn out to be remarkably small. Therefore, provided the effects of higher-order power corrections are small, the experimental determination of these two quantities is a very interesting tool for testing the SM and for investigating possible new physics.

*Email address: simula@roma3.infn.it

II. LIGHT-FRONT CALCULATION OF THE ISGUR-WISE FORM FACTOR

In this section we just briefly remind the main points of the light-front procedure for the calculation of the Λ_Q-type IW form factor $\xi(\omega)$ (see Ref. [2] for more general cases).

The spin structure of Λ_Q baryons can be represented by an antisymmetric (with respect to the two light quarks q and q') total spin-$\frac{1}{2}$ state [1]. In the so-called ''velocity basis'' the matrix elements of the vector current $J^\mu=\overline{Q}\gamma^\mu Q$ between Λ_Q states have the following form:

$$\mathcal{V}^\mu_{s's}\equiv\langle\Psi^{1/2s'}|\overline{Q}\gamma^\mu Q|\Psi^{1/2s}\rangle=F_1(\omega)\overline{u}(P',s')\gamma^\mu u(P,s)+[F_2(\omega)v^\mu+F_3(\omega)v'^\mu]\overline{u}(P',s')u(P,s), \tag{1}$$

where $u(P,s)$ is a Dirac spinor (normalized as $\overline{u}u=1$), $P=M_\Lambda v$ and $P'=P+q=M_\Lambda v'$, with M_Λ being the Λ-type baryon mass and q the four-momentum transfer. Since in Eq. (1) we are considering an elastic process, the four-momentum transfer squared is given by $q^2=2M_\Lambda^2(1-\omega)$ and has spacelike values ($q^2\leqslant 0$). In the heavy-quark limit ($m_Q\to\infty$) the following HQS relations hold [1]:

$$\lim_{m_Q\to\infty}F_1(\omega)=\xi(\omega),$$

$$\lim_{m_Q\to\infty}F_2(\omega)=\lim_{m_Q\to\infty}F_3(\omega)=0, \tag{2}$$

where the IW form factor $\xi(\omega)$ must satisfy the model-independent normalization $\xi(1)=1$ at the zero-recoil point $\omega=1$.

In the light-front formalism all the hadronic form factors corresponding to a conserved current can always be expressed in terms of the matrix elements of the *plus* component of the current, $J^+\equiv J^0+\hat{n}\cdot\vec{J}$ (where $\hat{n}$ is the spin-quantization axis); moreover, a reference frame where $q^+=0$ is adopted, which allows to suppress the contribution arising from the so-called Z-graph (pair creation from the vacuum) at any value of the heavy-quark mass. Thus, from Eq. (1) one easily gets

$$F_1(\omega)=\frac{1}{2}\mathrm{Tr}\left\{\frac{\mathcal{V}^+}{2P^+}\right\}+\frac{M_\Lambda}{\sqrt{-q^2}}\mathrm{Tr}\left\{\frac{\mathcal{V}^+ i\sigma_2}{2P^+}\right\}, \tag{3}$$

$$F_2(\omega)=F_3(\omega)=-\frac{M_\Lambda}{2\sqrt{-q^2}}\mathrm{Tr}\left\{\frac{\mathcal{V}^+ i\sigma_2}{2P^+}\right\}, \tag{4}$$

where $\widetilde{P}\equiv(P^+,\vec{P}_\perp)=\widetilde{p}_Q+\widetilde{p}_q+\widetilde{p}_{q'}$ is the LF baryon momentum (with $P^+=\sqrt{M_\Lambda^2-q^2/4}$) and $\widetilde{p}_i$ the quark one. Finally, the subscript $\perp$ indicates the projection perpendicular to the spin quantization axis.

Disregarding for simplicity the color and flavor degrees of freedom and limiting ourselves to S-wave baryons, the light-front Λ_Q wave function can be written as

$$\langle\{\xi_i\vec{k}_{i\perp};\sigma_i\}|\Psi^{1/2s}\rangle=\sqrt{\frac{E_Q E_q E_{q'}}{M_0\xi_Q\xi_q\xi_{q'}}}\sum_{\{\sigma_i'\}}\langle\{\sigma_i\}|\mathcal{R}^\dagger(\{\vec{k}_i;m_i\})|\{\sigma_i'\}\rangle\times\Phi^{1/2s}(\{\sigma_i'\})\;\; w_{(Qqq')}(\vec{p},\vec{k}), \tag{5}$$

where $\xi_i=p_i^+/P^+$ and $\vec{k}_{i\perp}=\vec{p}_{i\perp}-\xi_i\vec{P}_\perp$ are the intrinsic LF variables, $M_0^2=\Sigma_{i=Q,q,q'}(k_{i\perp}^2+m_i^2)/\xi_i$, $E_i=\sqrt{m_i^2+|\vec{k}_i|^2}$, with $\vec{k}_i\equiv(\vec{k}_{i\perp},k_{in})$ and $k_{in}=\frac{1}{2}(\xi_i M_0-(k_{i\perp}^2+m_i^2)/\xi_i M_0)$. Moreover, in Eq. (5) the curly braces $\{\ \}$ mean a list of indices corresponding to $i=Q,q,q'$; σ_i' indicates the third component of the quark spin; $\mathcal{R}(\{\vec{k}_i;m_i\})\equiv\Pi_{j=Q,q,q'}R_M(\vec{k}_j,m_j)$ is the product of the individual (generalized) Melosh rotations $R_M(\vec{k}_j,m_j)$. Finally, $\Phi^{1/2s}(\{\sigma_i'\})=\langle 1/2\sigma_Q',00|1/2s\rangle\ \langle 1/2\sigma_q',1/2\sigma_{q'}'|00\rangle$ is the canonical spin wave function and $w_{(Qqq')}(\vec{p},\vec{k})$ is the S-wave radial wave function, where

$$\vec{k}=(m_{q'}\vec{k}_q-m_q\vec{k}_{q'})/(m_q+m_{q'}),$$

$$\vec{p}=\frac{[(m_q+m_{q'})\vec{k}_Q-m_Q(\vec{k}_q+\vec{k}_{q'})]}{(m_Q+m_q+m_{q'})} \tag{6}$$

are the internal momenta conjugate, respectively, to the Jacobian coordinates

$$\vec{x}=\vec{r}_q-\vec{r}_{q'},$$

$$\vec{y}=\vec{r}_Q-(m_q\vec{r}_q+m_{q'}\vec{r}_{q'})/(m_q+m_{q'}). \tag{7}$$

In what follows we will consider two functional forms for the radial wave function, namely harmonic oscillator (h.o.) and power-law (p.l.) ones, viz.

$$w^{(h.o.)}_{(Qqq')}(\vec{p},\vec{k})=\left(\frac{1}{\pi\alpha_p}\right)^{3/4}e^{-|\vec{p}|^2/2\alpha_p^2}\left(\frac{1}{\pi\alpha_k}\right)^{3/4}e^{-|\vec{k}|^2/2\alpha_k^2}, \tag{8}$$

$$w^{(p.l.)}_{(Qqq')}(\vec{p},\vec{k})=\frac{N_p}{(\alpha_p^2+p^2)^{n_p}}\frac{N_k}{(\alpha_k^2+k^2)^{n_k}}, \tag{9}$$

where

$$N_{k(p)}\equiv\sqrt{4\Gamma[2n_{k(p)}]/\sqrt{\pi}\alpha_{k(p)}^{3-4n_{k(p)}}\Gamma\left[2n_{k(p)}-\frac{3}{2}\right]}$$

and $\Gamma(n)$ is the Euler Γ-function.

We have evaluated the right-hand side of Eqs. (3), (4) using the three-quark wave function given by Eq. (5) and adopting the h.o. (8) and p.l. (9) radial functions. The numerical integrations, involving six-dimensional integrals, have been performed through a well-established Monte Carlo procedure [5]. The heavy-quark limit ($m_Q\to\infty$) has been obtained by increasing the value of the heavy-quark mass until full convergence of the calculated form factors is reached.

We have found (see Ref. [2]) that the HQS relations (2) are satisfied at any value of ω. Thus, the IW form factor $\xi(\omega)$ is given by

$$\xi(\omega) = \frac{1}{2}\lim_{m_Q \to \infty} \mathrm{Tr}\left\{ \frac{\mathcal{V}^+}{2P^+} \right\}. \tag{10}$$

III. THE ISGUR-WISE FORM FACTOR AND THE BARYON STRUCTURE

The behavior of the calculated IW form factor $\xi(\omega)$ depends on the two parameters α_k and α_p, appearing in the radial wave functions (8), (9). To investigate such a dependence, let us consider the nonrelativistic baryon size r_B, defined as

$$r_B \equiv \sqrt{\langle r^2 \rangle_B} \equiv \sqrt{\sum_{i=Q,q,q'} \langle |\vec{r}_i - \vec{R}_{c.m.}|^2 \rangle}$$

$$\to_{m_Q \to \infty} \sqrt{\frac{1+\eta^2}{(1+\eta)^2}\langle x^2 \rangle + 2\langle y^2 \rangle}, \tag{11}$$

where $\eta \equiv m_q/m_{q'}$ and $\vec{R}_{c.m.} = \Sigma_{i=Q,q,q'} m_i \vec{r}_i / \Sigma_{i=Q,q,q'} m_i$. Since $\langle x^2 \rangle$ and $\langle y^2 \rangle$ are proportional to $1/\alpha_k^2$ and $1/\alpha_p^2$, respectively, the baryon size r_B can be easily written as a suitable combination of the parameters α_p and α_k. For instance, in the case of the h.o. wave function one immediately gets $r_B = \sqrt{3/\alpha_p^2 + (1+\eta^2)/(1+\eta)^2 (3/2\alpha_k^2)}$.

In the nonrelativistic limit the slope of the IW form factor at the zero-recoil point, $\rho_{IW}^2 \equiv -[d\xi(\omega)/d\omega]_{\omega=1}$, is proportional to the square of the baryon size r_B, so that when $\alpha_{k(p)} \to \infty$ one should have $\rho_{IW}^2 \to 0$. However, as suggested in Ref. [2], the relativistic delocalization of the light quark positions is expected to increase the slope ρ_{IW}^2 and the departure from the nonrelativistic behavior should appear when the baryon size r_B becomes much smaller than $\sqrt{\lambda_q^2 + \lambda_{q'}^2}$, where $\lambda_{q(q')} \equiv 1/m_{q(q')}$ is the constituent-quark Compton wavelength. For instance, putting $m_q = m_{q'} = 0.22$ GeV, the trigger value for the delocalization effects should be $r_B < 1.3$ fm.

The above relativistic effects are fully reflected in our light-front calculations for both the h.o. [2] and p.l. wave functions; in particular, we have found that the slope ρ_{IW}^2 is a monotonically decreasing function of $\alpha_{p(k)}$ and saturates when $\alpha_{p(k)}$ become large enough so that $r_B < \sqrt{\lambda_q^2 + \lambda_{q'}^2}$. The interesting point is that the saturation property holds not only for the slope ρ_{IW}^2 (i.e., at small recoils), but also for the IW form factor itself in the whole ω-range accessible in the decay $\Lambda_b \to \Lambda_c + l\bar{\nu}_l$ (i.e., $1 \leqslant \omega \lesssim 1.44$), as it is clearly illustrated in Fig. 1. Thus, in the saturation regime the IW form factor does not depend on the two parameters α_k and α_p separately, but only on one parameter, the ratio β, which we define as

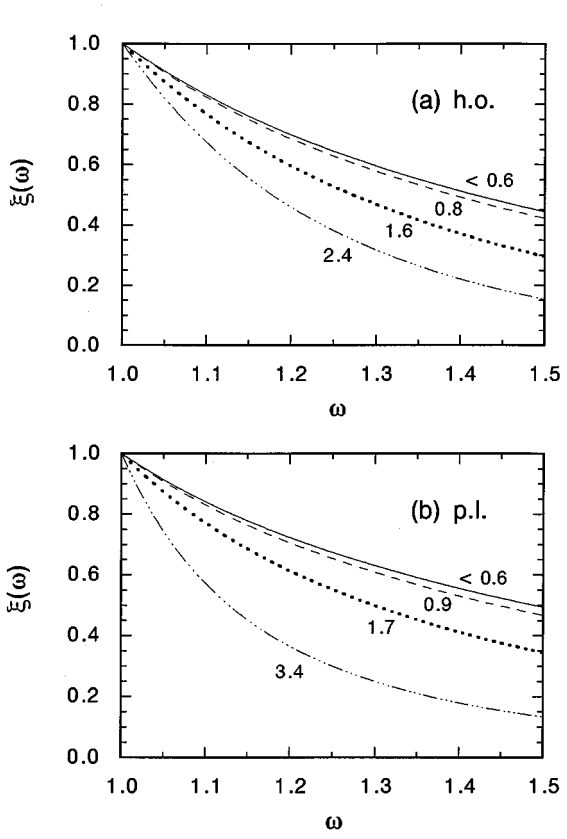

FIG. 1. The IW form factor $\xi(\omega)$ calculated using h.o. (a) and p.l. (b) wave functions versus ω [in (b) the value $n_p = n_k = 2$ has been considered]. The various lines correspond to different values of the parameter α_k, while the ratio β [Eq. (12)] is kept fixed at $\beta = 2$. For each curve the value of the baryon size r_B [Eq. (11)] in fm is reported. Finally, for the spectator-quark masses the value $m_q = m_{q'} = 0.22$ GeV is adopted.

$$\beta \equiv \sqrt{\frac{\langle |\vec{p}|^2 \rangle}{\langle |\vec{k}|^2 \rangle}} = \frac{\alpha_p}{\alpha_k} \quad \text{(h.o.)} = \frac{\alpha_p}{\alpha_k}\sqrt{\frac{4n_k - 5}{4n_p - 5}} \quad \text{(p.l.)}. \tag{12}$$

Since QCD is expected to confine hadrons within distances not larger than ~ 1 fm, we will consider in what follows to be in the saturation regime, where we stress the IW form factor depends only on the parameter β.[1] The physical meaning of this parameter has been already discussed in Ref. [2]. In coordinate space one gets $\beta^2 \sim \langle x^2 \rangle / \langle y^2 \rangle$ and, therefore, the two limiting cases, $\beta \ll 1$ and $\beta \gg 1$, correspond to a diquark-like and collinear-type configurations, respectively (see Fig. 2 of Ref. [2]). There is however still another parameter, namely the ratio of the light-quark masses $\eta = m_q/m_{q'}$. The sensitivity of the calculated IW function to the value of η is reported in Fig. 2. It can clearly be seen that in the light u,d,s spectator sector (where basically $0.5 \lesssim \eta$

[1] In practice, for any value of β we choose the value of the parameter α_k (or equivalently α_p) large enough so that $r_B \ll \sqrt{\lambda_q^2 + \lambda_{q'}^2}$

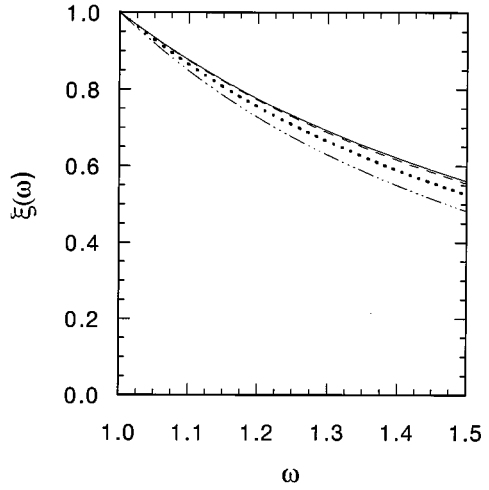

FIG. 2. The IW form factor $\xi(\omega)$ calculated for various values of the light-quark mass ratio $\eta=m_q/m_{q'}$. The value of β [Eq. (12)] is kept fixed at the value $\beta=4$ and the h.o. radial wave function [Eq. (8)] is considered. The solid, dashed, dotted and dot-dashed lines correspond to $\eta=1.00$, 0.52, 0.26 and 0.13, respectively.

$\leqslant 1$) there is no significant dependence of $\xi(\omega)$ on the particular value of η. This is not surprising, because in the saturation regime the IW form factor is dominated by relativistic effects, which means that the typical spectator-quark momenta are large compared with the spectator-quark masses and therefore the specific values of the latter play a minor role.

Let us now address the issue of the sensitivity of the calculated IW form factor to the choice of the Qqq' radial wave function. In Fig. 3 we show the IW function calculated at various values of β using the wave functions (8) and (9). It turns out that for each value of β the IW form factors corresponding to different radial wave functions are packed together in a narrow band, while the change in β affects more heavily the behavior of the IW form factor. Therefore we can state that within the ω-range accessible in the $\Lambda_b \to \Lambda_c + l\bar{\nu}_l$ decay ($1 \leqslant \omega \lesssim 1.44$) the ω-dependence of the IW function $\xi(\omega)$ is mainly governed by the value of only one parameter, β, and almost independent of the choice of the particular functional form of the radial wave function.

The above feature is relevant because any constraint on the value of β leads immediately to a constraint on the shape of the IW function $\xi(\omega)$ in the *full* ω-range. In other words, if our calculated IW function is expanded in a series of powers of $(\omega-1)$, the coefficients of this expansion are not independent of each other, but their values are related to the value of β. In order to constrain β our predictions for $\xi(\omega)$ corresponding to various values of β are compared in Fig. 4(a) with the recent lattice QCD results of Ref. [3], which have been obtained only at low values of the recoil. It can be seen that (i) there is a sharp sensitivity to the value of β, so that our predictions for $\xi(\omega)$ cover a quite large range of values; however, an upper bound on $\xi(\omega)$, corresponding to

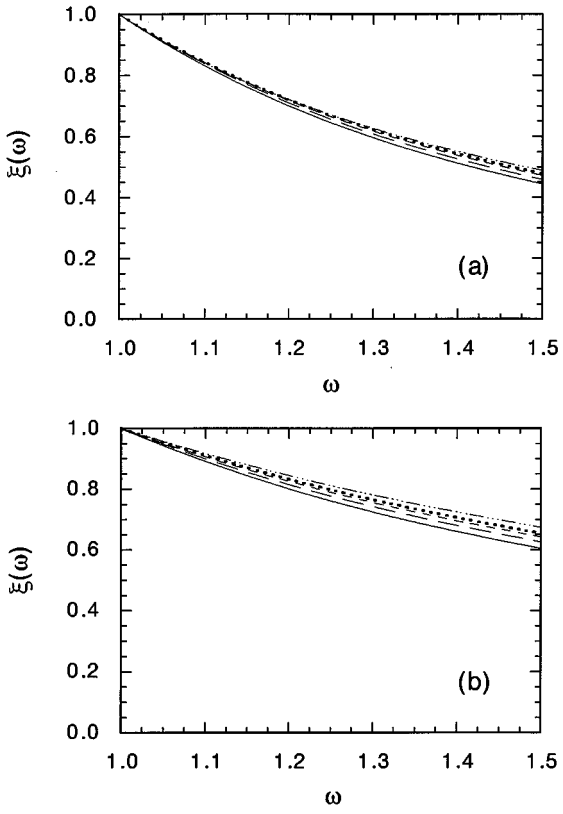

FIG. 3. The IW form factor $\xi(\omega)$ calculated at $\beta=2$ (a) and $\beta=10$ (b) using different baryon wave functions: h.o. (solid lines); p.l. with $n_p=n_k=2$, 3, 4 and 8 (dot-dashed, dotted, dashed and long-dashed lines, respectively).

$\beta \to \infty$ and represented by the solid line,[2] emerges in our LF quark model; (ii) only the calculations with $\beta \gtrsim 2$ can reproduce all the lattice points within the quoted errors. It should be noted that the above limits on β yield an allowed range for the IW function which is narrower than the spread of the lattice points themselves.

The same range of values for β is also suggested by the comparison with the results of Ref. [6], where dispersive bounds for the slope ρ^2_{IW} and the curvature $2c_{IW} \equiv [d^2\xi(\omega)/d\omega^2]_{\omega=1}$ of the Λ_Q-type IW form factor at the zero-recoil point have been derived. It should be mentioned however that the reliability of the dispersive bounds may be plagued by the effects of the so-called anomalous thresholds (see, e.g., Ref. [7]). With this *caveat* in mind, the theoretically allowed domain in the $\rho^2_{IW}-c_{IW}$ plane [6] is shown in Fig. 4(b) together with our results corresponding to various values of β. The dispersive bounds suggest a quite strong correlation among ρ^2_{IW} and c_{IW}, which is indeed reproduced in our calculations only for $\beta \gtrsim 2$. In conclusion, the results presented in Fig. 4 imply the dominance of collinear-type

[2]We have checked that the value $\beta=100$ is fully representative of the limiting case $\beta \to \infty$ for the calculation of the IW form factor $\xi(\omega)$.

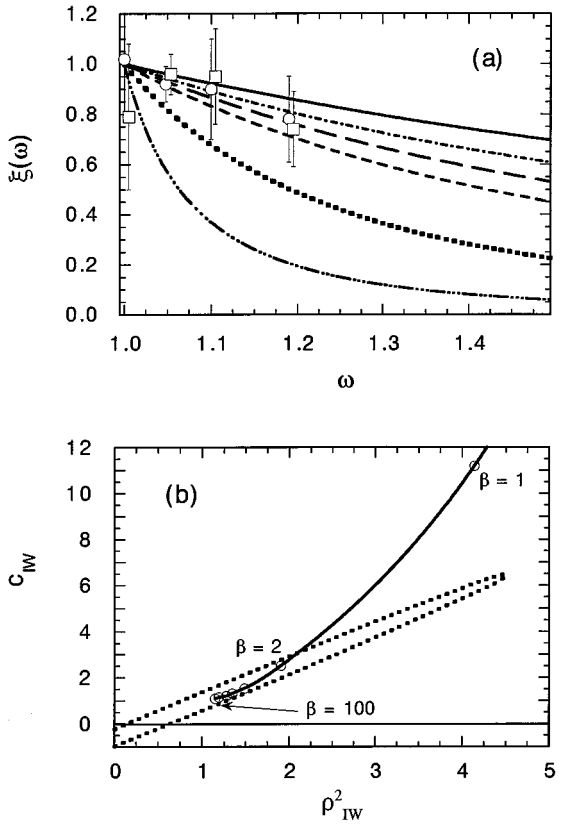

FIG. 4. (a) The IW function $\xi(\omega)$ calculated for different values of β and compared with the lattice QCD calculations of Ref. [3] (open dots and squares). The triple-dotted-dashed, dotted, dashed, long-dashed and dot-dashed lines correspond to $\beta=0.5$, 1.0, 2.0, 3.0 and 10.0, respectively, using the h.o. wave function (8). The solid line is the result obtained at $\beta=100$ using the p.l. wave function (9) with $n_p=n_k=2$. Adapted from Ref. [2]. (b) Curvature c_{IW} versus slope ρ^2_{IW} for the IW function $\xi(\omega)$. The dotted lines identify the allowed domain determined in Ref. [6]. The open dots correspond to our results obtained for various values of β and the solid line is just an interpolation curve.

configurations in the structure of Qqq' baryons.

In what follows we will estimate the model dependence due to the nonprecise knowledge of the Qqq' wave function using the results of the calculations of the IW form factor (10), obtained adopting the h.o. radial function (8) at $\beta=2$ and the p.l. function (9) with $n_p=n_k=2$ at $\beta=100$. These two form factors, which will be denoted by $\xi_L(\omega)$ and $\xi_U(\omega)$, represent our lower and upper bounds to the IW form factor $\xi(\omega)$, i.e., $\xi_L(\omega)\leqslant\xi(\omega)\leqslant\xi_U(\omega)$, corresponding to constrain the shape of $\xi(\omega)$ by the dashed and solid lines in Fig. 4(a). A simple polynomial fit for the ω-dependence of $\xi_L(\omega)$ and $\xi_U(\omega)$ can be found in the Appendix. From Eqs. (A1), (A2) of the Appendix the slope of the IW function at the zero-recoil point results to be $\rho^2_{IW}=1.35\pm0.55$.

IV. ANALYSIS OF THE $\Lambda_b \to \Lambda_c + l\bar{\nu}_l$ DECAY

The constraints on the shape of $\xi(\omega)$ obtained in the previous section can be used to reduce the model-dependence uncertainty in the evaluation of the (partially integrated) exclusive semileptonic branching ratio, defined as

$$Br_{\Lambda_b\to\Lambda_c l\bar{\nu}_l}(\omega_{\max}) \equiv \tau_{\Lambda_b}\int_1^{\omega_{max}} d\omega \frac{d\Gamma}{d\omega}(\Lambda_b\to\Lambda_c l\bar{\nu}_l), \tag{13}$$

where τ_{Λ_b} is the Λ_b mean lifetime ($\tau_{\Lambda_b}=1.24\pm0.08$ ps [8]) and $d\Gamma/d\omega$ is the differential decay rate for the $\Lambda_b\to\Lambda_c + l\bar{\nu}_l$ process. As for the latter, one has (see, e.g., Ref. [9])

$$\frac{d\Gamma}{d\omega}(\Lambda_b\to\Lambda_c l\bar{\nu}_l) = \frac{d\Gamma_L}{d\omega}(\Lambda_b\to\Lambda_c l\bar{\nu}_l) + \frac{d\Gamma_T}{d\omega}(\Lambda_b\to\Lambda_c l\bar{\nu}_l), \tag{14}$$

with the longitudinal (L) and transverse (T) parts given by

$$\frac{d\Gamma_L}{d\omega}(\Lambda_b\to\Lambda_c l\bar{\nu}_l) = \frac{G_F^2}{(2\pi)^3}|V_{bc}|^2 \frac{q^2 p_{\Lambda_c} M_{\Lambda_c}}{12 M_{\Lambda_b}}[|H_{1/2,0}|^2 + |H_{-1/2,0}|^2], \tag{15}$$

$$\frac{d\Gamma_T}{d\omega}(\Lambda_b\to\Lambda_c l\bar{\nu}_l) = \frac{G_F^2}{(2\pi)^3}|V_{bc}|^2 \frac{q^2 p_{\Lambda_c} M_{\Lambda_c}}{12 M_{\Lambda_b}}[|H_{1/2,1}|^2 + |H_{-1/2,-1}|^2], \tag{16}$$

where G_F is the Fermi coupling constant, V_{bc} is the relevant CKM matrix element and $p_{\Lambda_c}=M_{\Lambda_c}\sqrt{\omega^2-1}$ is the momentum of the daughter baryon Λ_c in the Λ_b rest frame. Within the SM the helicity amplitudes are given by

$$H_{\lambda_c,\lambda_W} = H^V_{\lambda_c,\lambda_W} - H^A_{\lambda_c,\lambda_W}, \tag{17}$$

where H^V and H^A are the vector (V) and axial-vector (A) helicity amplitudes, respectively, and λ_c and λ_W indicate the helicity of the daughter baryon and the one of the W-boson, respectively. The vector and axial-vector helicity amplitudes can be expressed in terms of the vector and axial-vector form factors as [9]

$$H^{V,A}_{1/2,1} = -2\sqrt{M_{\Lambda_b} M_{\Lambda_c}(\omega\mp1)}F_1^{V,A}(\omega),$$

$$H^{V,A}_{1/2,0} = \frac{1}{\sqrt{q^2}}\sqrt{2M_{\Lambda_b} M_{\Lambda_c}(\omega\mp1)}[(M_{\Lambda_b} \pm M_{\Lambda_c})F_1^{V,A}(\omega) \pm M_{\Lambda_c}(\omega\pm1)F_2^{V,A}(\omega) \pm M_{\Lambda_b}(\omega\pm1)F_3^{V,A}(\omega)], \tag{18}$$

where the upper and lower signs stand for the vector (V) and the axial-vector (A) case, respectively, and the amplitudes for negative values of the helicities can be obtained according to the relation $H^{V(A)}_{-\lambda_c,-\lambda_W} = +(-)H^{V(A)}_{\lambda_c,\lambda_W}$.

In the heavy-quark limit ($m_Q\to\infty$) one has

$$F_1^V(\omega) = F_1^A(\omega) = \xi(\omega),$$

$$F_{2,3}^V(\omega)=F_{2,3}^A(\omega)=0. \tag{19}$$

Including first-order $1/m_Q$ corrections to the HQS result (19) the six form factors $F_i^{V(A)}$ become [9]

$$\begin{aligned}
F_1^V(\omega)&=\xi(\omega)+\left(\frac{\Lambda}{2m_c}+\frac{\Lambda}{2m_b}\right)[2\chi(\omega)+\xi(\omega)],\\
F_2^V(\omega)&=-\frac{\Lambda}{m_c}\frac{\xi(\omega)}{1+\omega},\\
F_3^V(\omega)&=-\frac{\Lambda}{m_b}\frac{\xi(\omega)}{1+\omega},\\
F_1^A(\omega)&=\xi(\omega)+\left(\frac{\Lambda}{2m_c}+\frac{\Lambda}{2m_b}\right)\left[2\chi(\omega)+\xi(\omega)\frac{\omega-1}{\omega+1}\right],\\
F_2^A(\omega)&=-\frac{\Lambda}{m_c}\frac{\xi(\omega)}{1+\omega},\\
F_3^A(\omega)&=\frac{\Lambda}{m_b}\frac{\xi(\omega)}{1+\omega},
\end{aligned} \tag{20}$$

where $\Lambda\equiv M_{\Lambda_Q}-m_Q+O(1/m_Q)$ is the binding energy of the baryon in the heavy-quark limit and $\chi(\omega)$ is an (unknown) subleading function subject to the condition $\chi(1)=0$.

The effect of radiative corrections on the HQS relations (19) is to relate the vector and axial-vector form factors to the (renormalized) IW function $\xi(\omega)$ as follows (see, e.g., Ref. [10]):

$$\begin{aligned}
F_i^V(\omega)&=C_i^V(\omega)\xi(\omega),\\
F_i^A(\omega)&=C_i^A(\omega)\xi(\omega),
\end{aligned} \tag{21}$$

where $C_i^{V(A)}(\omega)$ with $i=1,\ 2,\ 3$ are renormalization-group invariant coefficients, which have been calculated and tabulated in Ref. [10]. A convenient parametrized form of the ω-dependence of all the six short-distance coefficients $C_i^{V(A)}(\omega)$ can be found in the Appendix. The inclusion of both radiative and $1/m_Q$ corrections leads to the following expressions [10]:

$$\begin{aligned}
F_1^V(\omega)&=C_1^V(\overline{\omega})\left\{\xi(\omega)+\left(\frac{\Lambda}{2m_c}+\frac{\Lambda}{2m_b}\right)[2\chi(\omega)+\xi(\omega)]\right\},\\
F_2^V(\omega)&=C_2^V(\overline{\omega})\xi(\omega)+\frac{\Lambda}{2m_b}C_2^V(\overline{\omega})\left[2\chi(\omega)+\xi(\omega)\frac{3\omega-1}{1+\omega}\right]+\frac{\Lambda}{2m_c}\left\{C_2^V(\overline{\omega})\left[2\chi(\omega)\right.\right.\\
&\quad\left.\left.+\xi(\omega)\frac{\omega-1}{1+\omega}\right]-\frac{2}{1+\omega}[C_1^V(\overline{\omega})+C_3^V(\overline{\omega})]\xi(\omega)\right\},\\
F_3^V(\omega)&=C_3^V(\overline{\omega})\xi(\omega)+\frac{\Lambda}{2m_c}C_3^V(\overline{\omega})\left[2\chi(\omega)+\xi(\omega)\frac{3\omega-1}{1+\omega}\right]+\frac{\Lambda}{2m_b}\left\{C_3^V(\overline{\omega})\left[2\chi(\omega)\right.\right.\\
&\quad\left.\left.+\xi(\omega)\frac{\omega-1}{1+\omega}\right]-\frac{2}{1+\omega}[C_1^V(\overline{\omega})+C_2^V(\overline{\omega})]\xi(\omega)\right\},\\
F_1^A(\omega)&=C_1^A(\overline{\omega})\left\{\xi(\omega)+\left(\frac{\Lambda}{2m_c}+\frac{\Lambda}{2m_b}\right)\left[2\chi(\omega)+\xi(\omega)\frac{\omega-1}{1+\omega}\right]\right\},\\
F_2^A(\omega)&=C_2^A(\overline{\omega})\xi(\omega)+\frac{\Lambda}{2m_b}C_2^A(\overline{\omega})\left[2\chi(\omega)+\xi(\omega)\frac{3\omega+1}{1+\omega}\right]+\frac{\Lambda}{2m_c}\left\{C_2^A(\overline{\omega})[2\chi(\omega)\right.\\
&\quad\left.+\xi(\omega)]-\frac{2}{1+\omega}[C_1^A(\overline{\omega})+C_3^A(\overline{\omega})]\xi(\omega)\right\},\\
F_3^A(\omega)&=C_3^A(\overline{\omega})\xi(\omega)+\frac{\Lambda}{2m_c}C_3^A(\overline{\omega})\left[2\chi(\omega)+\xi(\omega)\frac{3\omega+1}{1+\omega}\right]+\frac{\Lambda}{2m_b}\left\{C_3^A(\overline{\omega})[2\chi(\omega)\right.\\
&\quad\left.+\xi(\omega)]+\frac{2}{1+\omega}[C_1^A(\overline{\omega})-C_2^A(\overline{\omega})]\xi(\omega)\right\},
\end{aligned} \tag{22}$$

where $\overline{\omega}\equiv\omega+(\Lambda/m_b+\Lambda/m_c)(\omega-1)$.

In this work we calculate also various partially integrated asymmetries, namely the longitudinal $a_L(\omega_{max})$ and transverse $a_T(\omega_{max})$ asymmetries, defined as

$$a_L(\omega_{max}) = \frac{\int_1^{\omega_{max}} d\omega \;\; K(\omega) \;\; [|H_{1/2,0}|^2 - |H_{-1/2,0}|^2]}{\int_1^{\omega_{max}} d\omega \;\; K(\omega) \;\; [|H_{1/2,0}|^2 + |H_{-1/2,0}|^2]}, \tag{23}$$

$$a_T(\omega_{max}) = \frac{\int_1^{\omega_{max}} d\omega \;\; K(\omega) \;\; [|H_{1/2,1}|^2 - |H_{-1/2,-1}|^2]}{\int_1^{\omega_{max}} d\omega \;\; K(\omega) \;\; [|H_{1/2,1}|^2 + |H_{-1/2,-1}|^2]}, \tag{24}$$

where $K(\omega) \equiv [G_F^2/(2\pi)^3]|V_{bc}|^2 (q^2 p_{\Lambda_c} M_{\Lambda_c}/12 M_{\Lambda_b})$, and the ratio of the longitudinal to transverse decay rates $R_{L/T}(\omega_{max})$, viz.

$$R_{L/T}(\omega_{max}) = \frac{\int_1^{\omega_{max}} d\omega \;\; \frac{d\Gamma_L}{d\omega}(\Lambda_b \to \Lambda_c l \bar{\nu}_l)}{\int_1^{\omega_{max}} d\omega \;\; \frac{d\Gamma_T}{d\omega}(\Lambda_b \to \Lambda_c l \bar{\nu}_l)}. \tag{25}$$

Finally, the (partially integrated) longitudinal Λ_c polarization $P_L(\omega_{max})$ (as defined in Ref. [9]) can be easily obtained in terms of $a_L(\omega_{max})$, $a_T(\omega_{max})$ and $R_{L/T}(\omega_{max})$ as

$$P_L(\omega_{max}) = \frac{a_T(\omega_{max}) + a_L(\omega_{max}) \;\; R_{L/T}(\omega_{max})}{1 + R_{L/T}(\omega_{max})}. \tag{26}$$

Note that within the SM all the various observables (23)–(26) are independent of the specific value (and uncertainty) of $|V_{bc}|$.

We have evaluated the exclusive semileptonic branching ratio (13) and the various observables given by Eqs. (23)–(26), using the expressions (19)–(22) for the relevant form factors entering the helicity amplitudes (18) and adopting the two IW functions $\xi_L(\omega)$ and $\xi_U(\omega)$, determined in the previous section. Up to first-order $1/m_Q$ corrections, the values of the quark masses m_b and m_c are given by $m_b = M_{\Lambda_b} - \Lambda$ and $m_c = M_{\Lambda_c} - \Lambda$, with $M_{\Lambda_b} = 5.624$ GeV and $M_{\Lambda_c} = 2.285$ GeV from the Particle Data Group (PDG) [8]. Thus, in Eqs. (20) and (22) there are only two unknowns, the subleading function $\chi(\omega)$ and the baryonic binding energy Λ. In Ref. [3] the m_Q dependence of the lattice QCD results has been investigated, obtaining that the value $\Lambda = 0.75^{+10\,+5}_{-13\,-6}$ GeV and $\chi(\omega) \simeq 0$ are consistent with the lattice points. Moreover, the subleading function $\chi(\omega)$ has been recently calculated using QCD sum rules in Ref. [11] and within the quark model of Ref. [12]. In both calculations the resulting $\chi(\omega)$ turns out to be quite small (of the order of a few percent); in particular it has been found to be negative in [11], while both positive and negative subleading functions have been obtained in [12] according to the values adopted for the quark-model parameters. Thus, we have calculated the exclusive semileptonic branching ratio and the various asymmetries using for $\chi(\omega)$ the results labeled *I* in Ref. [11], but considering either a positive or a negative sign. It turns out that the branching ratio is modified by about $\pm 2\%$, while the effect on the asymmetries is well below $\pm 1\%$. Therefore, in what follows we adopt the approximation $\chi(\omega) = 0$ and inflate the theoretical error of the calculated branching ratio by adding a $\pm 2\%$ uncertainty.

We have first investigated the sensitivity of the observables (13) and (23)–(26), integrated in the whole ω-range accessible in $\Lambda_b \to \Lambda_c + l\bar{\nu}_l$ [i.e., for $\omega_{max} = \omega_{th} = (M_{\Lambda_b}^2 + M_{\Lambda_c}^2)/2M_{\Lambda_b}M_{\Lambda_c} \simeq 1.44$], to the radiative corrections in the heavy-quark limit [see Eqs. (21)]. Our predictions, corresponding to the average $\pm$ the semidispersion of the results obtained using $\xi(\omega) = \xi_L(\omega)$ and $\xi(\omega) = \xi_U(\omega)$, are reported in Table I. It can clearly be seen that PQCD corrections lower $Br(\Lambda_b \to \Lambda_c l \bar{\nu}_l) \equiv Br_{\Lambda_b \to \Lambda_c l \bar{\nu}_l}(\omega_{th})$ and $a_T \equiv a_T(\omega_{th})$ by about 10%, while the other asymmetries $a_L \equiv a_L(\omega_{th})$ and $P_L \equiv P_L(\omega_{th})$ as well as the ratio $R_{L/T} \equiv R_{L/T}(\omega_{th})$ are only marginally modified.

Then, since the HQET parameter Λ governs the strength of the $1/m_Q$ corrections, we have investigated the sensitivity of the (totally integrated) exclusive semileptonic branching ratio and asymmetries to the specific value of Λ both with and without radiative corrections [see Eqs. (22) and (20), respectively]. Our predictions are reported in Tables II and

TABLE I. Results for the (totally integrated) exclusive semileptonic branching ratio $Br(\Lambda_b \to \Lambda_c l \bar{\nu}_l)$ [in % at $|V_{bc}|=0.040$ and $\tau(\Lambda_b)=1.24$ ps [8]], the longitudinal a_L and transverse a_T asymmetries, the longitudinal daughter-baryon polarization P_L and the longitudinal to transverse ratio $R_{L/T}$ obtained for the decay process $\Lambda_b \to \Lambda_c + l \bar{\nu}_l$ in the HQS limit ($m_Q \to \infty$) without and with radiative corrections [see Eqs. (19) and (21), respectively]. The values reported are the average and the semidispersion of the results obtained using $\xi(\omega)=\xi_L(\omega)$ and $\xi(\omega)=\xi_U(\omega)$ (see text and Appendix).

	$Br(\%)$	a_L	a_T	P_L	$R_{L/T}$
HQS	6.65 ± 1.41	-0.931 ± 0.009	-0.488 ± 0.012	-0.763 ± 0.018	1.63 ± 0.12
HQS + PQCD	6.07 ± 1.27	-0.939 ± 0.009	-0.539 ± 0.012	-0.785 ± 0.018	1.61 ± 0.12

III. It can clearly be seen that the first-order $1/m_Q$ corrections yield an increase of the calculated $Br(\Lambda_b \to \Lambda_c l \bar{\nu}_l)$ (about 10% at $\Lambda=0.75$ GeV), which is partially compensated by a corresponding decrease due to radiative corrections. Thus, radiative plus first-order power corrections affect only marginally the exclusive semileptonic branching ratio, so that the model dependence turns out to be the most important source of uncertainty on $Br(\Lambda_b \to \Lambda_c l \bar{\nu}_l)$, the longitudinal asymmetry a_L is only slightly sensitive to both radiative and $1/m_Q$ corrections, the effects of radiative and $1/m_Q$ corrections are opposite in the longitudinal to transverse decay ratio $R_{L/T}$, but the total effect is smaller than the uncertainty due to the model dependence, and the transverse asymmetry a_T and the longitudinal Λ_c polarization P_L are remarkably affected by radiative and $1/m_Q$ corrections, while their model dependence is quite smaller.

Similar conclusions hold as well also for the partially integrated observables at $\omega_{max} < \omega_{th}$, as it can be seen in Table IV in the case of the exclusive semileptonic branching ratio $Br_{\Lambda_b \to \Lambda_c l \bar{\nu}_l}(\omega_{max})$ (see also Fig. 6 later on). Therefore, taking into account both the model dependence and the sensitivity to the $1/m_Q$ corrections in the whole range of values $0 \leqslant \Lambda(\mathrm{GeV}) \leqslant 1$, our final predictions (including radiative corrections) are $Br(\Lambda_b \to \Lambda_c l \bar{\nu}_l)=(6.3 \pm 1.6)\% \, |V_{bc}/0.040|^2 \, \tau(\Lambda_b)/(1.24 \text{ ps})$, $a_L=-0.945 \pm 0.014$, $a_T=-0.62 \pm 0.09$ and $R_{L/T}=1.57 \pm 0.15$. The corresponding result for the longitudinal Λ_c polarization is $P_L=-0.82 \pm 0.05$.

In Fig. 5 the upper [corresponding to $\xi(\omega)=\xi_U(\omega)$] and lower [corresponding to $\xi(\omega)=\xi_L(\omega)$] results for the partially integrated exclusive semileptonic branching ratio $Br_{\Lambda_b \to \Lambda_c l \bar{\nu}_l}(\omega_{max})$, obtained adopting the value $\Lambda=0.75$ GeV in Eq. (22), are shown and compared with the HQS results [Eqs. (19)] and with the lattice predictions of Ref. [3]. It can be seen that our results are always well within the range of values given by the lattice QCD simulations and that radiative plus first-order power corrections modify only slightly the HQS results. If the integration over the recoil is limited to $\omega_{max}=1.2$, then the resulting uncertainty on $Br_{\Lambda_b \to \Lambda_c l \bar{\nu}_l}(\omega_{max})$ reduces significantly to $\simeq 12\%$, though at the price of reducing the number of the events by a factor $\simeq 0.44$ (see Table II). This implies the possibility to extract the CKM matrix elements $|V_{bc}|$ with a theoretical uncertainty of $\simeq 6\%$, which is comparable with present uncertainties obtained from exclusive semileptonic B-meson decays [4].

The dependence of the various asymmetries (23)–(26) upon ω_{max} is illustrated in Table V and in Fig. 6, where the lattice predictions [3] for $R_{L/T}(\omega_{max})$ are also reported. All the observables considered do depend on the specific value of ω_{max}, so that in comparing with (future) data the precise ω-range of the experiments has to be taken into account. In Fig. 6 the HQS results are also shown for each observable. It turns out that radiative plus first-order $1/m_Q$ corrections are relevant for the transverse asymmetry $a_T(\omega_{max})$ and for the longitudinal Λ_c polarization $P_L(\omega_{max})$ at any value of ω_{max},

TABLE II. Results for the (totally integrated) exclusive semileptonic branching ratio $Br(\Lambda_b \to \Lambda_c l \bar{\nu}_l)$ [in % at $|V_{bc}|=0.040$ and $\tau(\Lambda_b)=1.24$ ps [8]], the longitudinal a_L and transverse a_T asymmetries, the longitudinal daughter-baryon polarization P_L and the longitudinal to transverse ratio $R_{L/T}$ obtained at different values of the binding energy Λ without including radiative corrections [see Eqs. (20)]. For the meaning of the errors see Table I.

Λ (GeV)	$Br(\%)$	a_L	a_T	P_L	$R_{L/T}$
0.00	6.65 ± 1.41	-0.931 ± 0.009	-0.488 ± 0.012	-0.763 ± 0.018	1.63 ± 0.12
0.25	6.81 ± 1.45	-0.934 ± 0.009	-0.521 ± 0.012	-0.777 ± 0.018	1.63 ± 0.12
0.50	7.03 ± 1.51	-0.937 ± 0.009	-0.559 ± 0.013	-0.793 ± 0.017	1.64 ± 0.12
0.75	7.35 ± 1.58	-0.942 ± 0.008	-0.604 ± 0.013	-0.814 ± 0.016	1.65 ± 0.12
1.00	7.82 ± 1.70	-0.948 ± 0.008	-0.658 ± 0.013	-0.839 ± 0.015	1.67 ± 0.12

TABLE III. The same as in Table II, but including radiative corrections [see Eqs. (22)]. For the meaning of the errors see Table I.

Λ (GeV)	$Br(\%)$	a_L	a_T	P_L	$R_{L/T}$
0.00	6.07 ± 1.27	-0.939 ± 0.009	-0.539 ± 0.013	-0.785 ± 0.017	1.61 ± 0.12
0.25	6.11 ± 1.27	-0.941 ± 0.008	-0.571 ± 0.013	-0.798 ± 0.017	1.59 ± 0.12
0.50	6.18 ± 1.29	-0.943 ± 0.008	-0.604 ± 0.013	-0.812 ± 0.016	1.57 ± 0.11
0.75	6.28 ± 1.31	-0.946 ± 0.008	-0.651 ± 0.013	-0.830 ± 0.015	1.55 ± 0.11
1.00	6.44 ± 1.34	-0.950 ± 0.007	-0.701 ± 0.013	-0.851 ± 0.013	1.53 ± 0.11

whereas both $a_L(\omega_{max})$ and $R_{L/T}(\omega_{max})$ are only marginally affected by radiative plus first-order power corrections. Moreover, the model dependence on the various asymmetries is generally quite limited and it reduces as ω_{max} decreases. In particular, our uncertainty on $R_{L/T}(\omega_{max})$, which is always much less than the one presently achievable by lattice QCD calculations, reduces to $\simeq 1\%$ at $\omega_{max} = 1.2$. To sum up, both the longitudinal asymmetry $a_L(\omega_{th})$ and the longitudinal to transverse decay ratio $R_{L/T}(\omega_{max} \simeq 1.2)$ represent very interesting quantities to be determined experimentally in order to test the SM and to investigate possible new physics.

All the conclusions obtained so far are based on Eqs. (22) for the form factors, i.e., on the inclusion of power corrections up to first order in $1/m_Q$. The second-order power corrections to F_1^A and $F_1^V + F_2^V + F_3^V$ at the zero-recoil point have been estimated in Ref. [13] and found to be of the order of a few percent. In the case of the $B \to D^*(D)$ transitions important effects of second-order power corrections may be present (see, e.g., Ref. [14]); however, a (model-dependent) analysis [15] of $1/m_Q^2$ corrections in mesons and baryons suggests that smaller corrections can be expected in the $\Lambda_b \to \Lambda_c$ transition with respect to the $B \to D^*(D)$ case, thanks to the absence of hyperfine splitting effects related to the finite mass of the charm quark. Nevertheless, we feel it is mandatory to check that our findings (particularly those for the asymmetries) still survive after the inclusion of second-order power corrections.

Before closing this section, we want to present our estimates of the exclusive semileptonic branching ratio and the asymmetries for the decay process $\Xi_b \to \Xi_c + l\bar{\nu}_l$, where the light spectator quarks are a us (ds) pair. As already illustrated in Fig. 2, we do not expect that the IW form factor is modified significantly by the presence of the s quark mass instead of the $u(d)$ one; this does not imply that the IW form factors for Λ_Q- and Ξ_Q-type baryons are the same, because of possible differences in the radial wave functions in the two heavy systems. In the absence of a more precise knowledge of $SU(3)$ breaking effects, we assume the same range of variation of the parameter β, i.e., $\beta \gtrsim 2$. Moreover, both the binding energy $\Lambda^{(s)}$ and the physical threshold $\omega_{th}^{(s)} = (M_{\Xi_b}^2 + M_{\Xi_c}^2)/2M_{\Xi_b}M_{\Xi_c}$ have to be determined. Since the

TABLE IV. Values of the (partially integrated) exclusive semileptonic branching ratio $Br_{\Lambda_b \to \Lambda_c l\bar{\nu}_l}(\omega_{max})$ in % versus ω_{max} [see Eq. (13)], calculated at $|V_{bc}| = 0.040$ and $\tau(\Lambda_b) = 1.24$ ps [8] for the decay process $\Lambda_b \to \Lambda_c + l\bar{\nu}_l$. The columns labelled HQS, HQS+PQCD, HQS+$1/m_Q$ and HQS+PQCD+$1/m_Q$ correspond to the heavy-quark limit $m_Q \to \infty$ [Eqs. (19)], to the inclusion of radiative corrections [Eqs. (21)] and of the first-order $1/m_Q$ corrections, as given by Eqs. (20) and (22) with $\Lambda = 0.75$ GeV, respectively. For the meaning of the errors see Table I.

ω_{max}	HQS	HQS+PQCD	HQS+$1/m_Q$	HQS+PQCD+$1/m_Q$
1.05	0.43 ± 0.01	0.42 ± 0.01	0.44 ± 0.01	0.43 ± 0.01
1.10	1.15 ± 0.07	1.10 ± 0.07	1.19 ± 0.07	1.13 ± 0.07
1.15	1.97 ± 0.17	1.88 ± 0.17	2.08 ± 0.19	1.94 ± 0.17
1.20	2.84 ± 0.33	2.69 ± 0.31	3.03 ± 0.35	2.79 ± 0.32
1.25	3.72 ± 0.52	3.49 ± 0.48	4.01 ± 0.56	3.64 ± 0.50
1.30	4.57 ± 0.74	4.26 ± 0.68	4.97 ± 0.81	4.44 ± 0.71
1.35	5.39 ± 0.98	4.99 ± 0.89	5.90 ± 1.09	5.19 ± 0.93
1.40	6.16 ± 1.24	5.65 ± 1.12	6.79 ± 1.38	5.87 ± 1.16
1.44	6.65 ± 1.41	6.07 ± 1.27	7.35 ± 1.58	6.28 ± 1.31

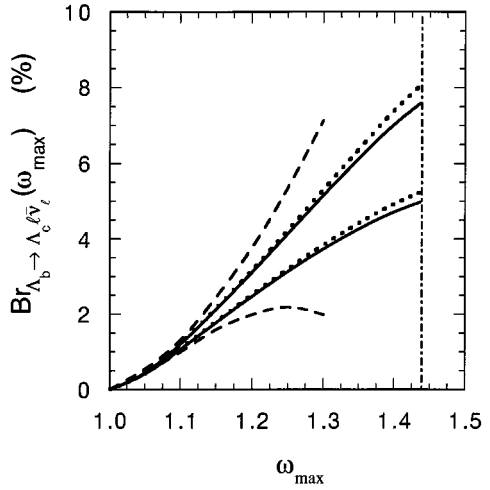

FIG. 5. Partially integrated exclusive semileptonic branching ratio $Br_{\Lambda_b\to\Lambda_c l\bar{\nu}_l}(\omega_{max})$ in % versus ω_{max} [see Eq. (13)], calculated at $|V_{bc}|=0.040$ and $\tau(\Lambda_b)=1.24$ ps [8] for the decay process $\Lambda_b\to\Lambda_c+l\bar{\nu}_l$. The solid and dashed lines correspond to our and lattice QCD results [3], respectively. The lower and upper solid lines are the results corresponding to the use of $\xi(\omega)=\xi_L(\omega)$ and $\xi(\omega)=\xi_U(\omega)$ in Eq. (22), respectively, i.e., including radiative plus first-order $1/m_Q$ corrections with $\Lambda=0.75$ GeV. The dotted lines are the HQS results [see Eqs. (19)]. The vertical dot-dashed line indicates the physical threshold $\omega_{th}\simeq 1.44$.

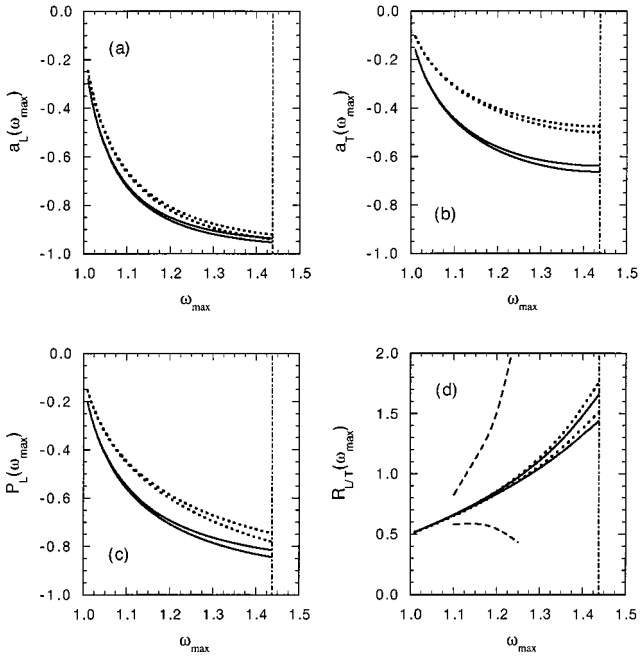

FIG. 6. Partially integrated longitudinal asymmetry $a_L(\omega_{max})$ (a), transverse asymmetry $a_T(\omega_{max})$ (b), longitudinal daughter-baryon polarization $P_L(\omega_{max})$ (c) and longitudinal to transverse decay ratio $R_{L/T}(\omega_{max})$ (d) versus ω_{max} for the decay process $\Lambda_b\to\Lambda_c+l\bar{\nu}_l$. The dotted and solid lines correspond to the results obtained in the heavy-quark limit [see Eqs. (19)] and using Eqs. (22) with $\Lambda=0.75$ GeV, respectively. The lower and upper lines are the results corresponding to $\xi(\omega)=\xi_L(\omega)$ and $\xi(\omega)=\xi_U(\omega)$, respectively. In (d) the dashed lines correspond to the lattice QCD results of Ref. [3]. The vertical dot-dashed lines indicate the physical threshold $\omega_{th}\simeq 1.44$.

c quark mass should be the same in the two decay processes $\Lambda_b\to\Lambda_c+l\bar{\nu}_l$ and $\Xi_b\to\Xi_c+l\bar{\nu}_l$, we assume $M_{\Lambda_c}-\Lambda=M_{\Xi_c}-\Lambda^{(s)}$. Using the experimental value $M_{\Xi_c}=2.466$ GeV [8] we get $\Lambda^{(s)}=0.931$ GeV. In an analogous way for the b-quark case, we consider that $M_{\Lambda_b}-\Lambda=M_{\Xi_b}$

TABLE V. Values of the (partially integrated) asymmetries $a_L(\omega_{max})$ [Eq. (23)] and $a_T(\omega_{max})$ [Eq. (4)], the longitudinal daughter-baryon polarization $P_L(\omega_{max})$ [Eq. (26)] and the (partially integrated) ratio of longitudinal to transverse decay rate $R_{L/T}(\omega_{max})$ [Eq. (25)] versus ω_{max} for the decay process $\Lambda_b\to\Lambda_c+l\bar{\nu}_l$. Both the radiative and the first-order $1/m_Q$ corrections, given by Eqs. (22) with $\Lambda=0.75$ GeV, are included. For the meaning of the errors see Table I.

ω_{max}	a_L	a_T	P_L	$R_{L/T}$
1.01	-0.282 ± 0.001	-0.159 ± 0.001	-0.201 ± 0.001	0.515 ± 0.001
1.05	-0.571 ± 0.002	-0.338 ± 0.001	-0.423 ± 0.002	0.576 ± 0.001
1.10	-0.725 ± 0.004	-0.451 ± 0.003	-0.557 ± 0.006	0.657 ± 0.002
1.15	-0.808 ± 0.005	-0.521 ± 0.005	-0.643 ± 0.006	0.745 ± 0.005
1.20	-0.858 ± 0.006	-0.569 ± 0.007	-0.701 ± 0.007	0.842 ± 0.011
1.25	-0.891 ± 0.007	-0.603 ± 0.009	-0.743 ± 0.009	0.951 ± 0.019
1.30	-0.913 ± 0.007	-0.626 ± 0.010	-0.775 ± 0.011	1.088 ± 0.032
1.35	-0.929 ± 0.008	-0.641 ± 0.012	-0.800 ± 0.012	1.226 ± 0.051
1.40	-0.940 ± 0.008	-0.649 ± 0.013	-0.819 ± 0.014	1.404 ± 0.081
1.44	-0.946 ± 0.008	-0.651 ± 0.013	-0.830 ± 0.015	1.548 ± 0.110

$-\Lambda^{(s)}$; using the previously determined value of $\Lambda^{(s)}$, we get $M_{\Xi_b}=5.805$ GeV, which is in reasonable overall agreement with the lattice QCD results $5.76^{+3\,+4}_{-5\,-3}$ GeV from Ref. [16]. Finally, from the obtained values of the Ξ_Q-type baryon masses one has $\omega_{th}^{(s)} \simeq 1.39$. Thus, after including radiative plus first-order $1/m_Q$ corrections (22) to the relevant form factors our estimates are $Br(\Xi_b \to \Xi_c l\bar{\nu}_l)=(7.9\pm 2.0)\%$ [at $|V_{bc}|=0.040$ and $\tau(\Xi_b)=1.39$ ps [8]], $a_L(\Xi_b \to \Xi_c l\bar{\nu}_l) = -0.947 \pm 0.013$, $a_T(\Xi_b \to \Xi_c l\bar{\nu}_l) = -0.62 \pm 0.11$, $P_L(\Xi_b \to \Xi_c l\bar{\nu}_l) = -0.87 \pm 0.05$ and $R_{L/T}(\Xi_b \to \Xi_c l\bar{\nu}_l) = 1.60 \pm 0.14$.

V. CONCLUSIONS

The Isgur-Wise form factor relevant for the $\Lambda_b \to \Lambda_c + l\bar{\nu}_l$ semileptonic decay has been calculated in the whole accessible kinematical range adopting a light-front constituent quark model and using various forms of the Qqq' wave function. It has been shown that the IW form factor is sensitive to light-quark relativistic delocalization effects, leading to a saturation property of the form factor as a function of the (nonrelativistic) baryon size (11). Moreover, the behavior of the IW function turns out to be largely affected by the baryon structure, being sharply different in the case of diquark or collinear-type Qqq' configurations. The comparison with recent lattice QCD calculations [3] at low recoil suggests the dominance of collinear-type configurations with respect to diquark-like ones and allows to put effective constraints on the shape of the IW function in the full ω-range. Then, the $\Lambda_b \to \Lambda_c + l\bar{\nu}_l$ decay has been investigated including both radiative and first-order $1/m_Q$ corrections to the relevant form factors. Our final predictions for the exclusive semileptonic branching ratio, the longitudinal and transverse asymmetries, and the longitudinal to transverse decay ratio are $Br(\Lambda_b \to \Lambda_c l\bar{\nu}_l)=(6.3\pm 1.6)\%|V_{bc}/0.040|^2 \tau(\Lambda_b)/(1.24\ \text{ps})$, $a_L = -0.945 \pm 0.014$, $a_T = -0.62 \pm 0.09$ and $R_{L/T}=1.57\pm 0.15$, respectively. It has also been shown that the theoretical uncertainties on $Br(\Lambda_b \to \Lambda_c l\bar{\nu}_l)$ and $R_{L/T}$ can be significantly reduced to $\simeq 12\%$ and $\simeq 1\%$, respectively, by integrating the differential decay rates up to $\omega \simeq 1.2$. This could allow the extraction of the CKM matrix elements $|V_{bc}|$ with a theoretical uncertainty of $\simeq 6\%$, which is comparable with present uncertainties obtained from exclusive semileptonic B-meson decays. Finally, we stress that, provided the effects of higher-order power corrections are negligible, the small uncertainties found for the longitudinal asymmetry and the (partially integrated) longitudinal to transverse decay ratio make the experimental determination of these quantities a very interesting tool for testing the SM and investigating possible new physics.

APPENDIX

The results of the calculations of the form factors $\xi_L(\omega)$ and $\xi_U(\omega)$ (see Sec. III), performed in the whole ω-range accessible in the decay $\Lambda_b \to \Lambda_c + l\bar{\nu}_l$, can be fitted with high accuracy by the following quartic polynomials in the recoil variable $\omega - 1$, viz.

$$\xi_{L(U)}(\omega) = 1 - \hat{\rho}^2_{L(U)}(\omega-1) + \hat{c}_{L(U)}(\omega-1)^2 - \hat{d}_{L(U)}(\omega-1)^3 + \hat{f}_{L(U)}(\omega-1)^4, \tag{A1}$$

where the values of the parameters are

$$\hat{\rho}^2_L = 1.884, \quad \hat{c}_L = 2.241, \quad \hat{d}_L = 1.626, \quad \hat{f}_L = 0.5143,$$

$$\hat{\rho}^2_U = 0.8252, \quad \hat{c}_U = 0.5388, \quad \hat{d}_U = 0.2594, \quad \hat{f}_U = 0.06308. \tag{A2}$$

We stress that neither a linear nor a quadratic polynomial is able to reproduce accurately the ω-behavior of the form factors $\xi_L(\omega)$ and $\xi_U(\omega)$ in the whole range of values of the recoil accessible in the decay $\Lambda_b \to \Lambda_c + l\bar{\nu}_l$.

The results of the calculations of the short-distance coefficients $C_i^{V(A)}(\omega)$ reported in Ref. [10] can be fitted for $\omega \lesssim 1.8$ as follows:

$$C_1^V(\omega) = 1.136 - 0.2978(\omega-1) + 0.01149(\omega-1)^2 - 0.03536(\omega-1)^3,$$

$$C_2^V(\omega) = -0.08485 + 0.04645(\omega-1) - 0.02792(\omega-1)^2 + 0.01263(\omega-1)^3,$$

$$C_3^V(\omega) = -0.02133 + 0.007972(\omega-1) - 0.001840(\omega-1)^2 \tag{A3}$$

and

$$C_1^A(\omega) = 0.9851 - 0.2069(\omega-1) + 0.04899(\omega-1)^2 - 0.001684(\omega-1)^3,$$

$$C_2^A(\omega) = -0.1220 + 0.07378(\omega-1) - 0.04062(\omega-1)^2 + 0.01347(\omega-1)^3,$$

$$C_3^A(\omega) = 0.04203 - 0.02193(\omega-1) + 0.008658(\omega-1)^2. \tag{A4}$$

[1] N. Isgur and M.B. Wise, Nucl. Phys. **B348**, 276 (1991).
[2] F. Cardarelli and S. Simula, Phys. Lett. B **421**, 295 (1998); and in Proceedings of the III International Conference on *Quark Confinement and the Hadron Structure*, Jefferson Lab, 1998 (in press).
[3] UKQCD Collaboration, K.C. Bowler *et al.*, Phys. Rev. D **57**, 6948 (1998).
[4] For an updated analysis of the theoretical uncertainties affecting the extraction of V_{bc}, see I.I. Bigi *et al.*, Annu. Rev. Nucl. Part. Sci. **47**, 591 (1997).
[5] G.P. Lepage, J. Comput. Phys. **27**, 192 (1978).
[6] D. Chakraverty, T. De, B. Dutta-Roy, and K.S. Gupta, SINP-TNP-98-04, e-print archive hep-ph/9802223.
[7] C.E. Carlson *et al.*, Phys. Lett. B **299**, 133 (1993); C.A. Dominguez, J.K. Körner, and D. Pirjol, *ibid.* **301**, 257 (1993); B. Holdom and M. Sutherland, Z. Phys. C **65**, 445 (1995).
[8] Particle Data Group, C. Caso *et al.*, Eur. Phys. J. C **3**, 1 (1998).
[9] J.G. Korner *et al.*, Prog. Part. Nucl. Phys. **33**, 787 (1994).
[10] M. Neubert, Phys. Rep. **245**, 259 (1994).
[11] Y. Dai, C. Huang, M. Huang, and C. Liu, Phys. Lett. B **387**, 379 (1996).
[12] B. König, J.G. Körner, M. Krämer, and P. Kroll, Phys. Rev. D **56**, 4282 (1997).
[13] J.G. Körner and D. Pirjol, Phys. Lett. B **334**, 399 (1994).
[14] B. Holdom and M. Sutherland, Phys. Rev. D **47**, 5067 (1993); Phys. Lett. B **313**, 447 (1993); Phys. Rev. D **48**, 5196 (1993).
[15] B. Holdom, M. Sutherland, and J. Mureika, Phys. Rev. D **49**, 2359 (1994).
[16] UKQCD Collaboration, K.C. Bowler *et al.*, Phys. Rev. D **54**, 3619 (1996).